

Supplementary information

Data-driven design of dual-metal-site catalysts for electrochemical carbon dioxide reduction reaction

Haisong Feng[‡], Hu Ding[‡], Peinan He, Si Wang, Zeyang Li, Zikang Zheng, Yusen Yang,* Min Wei
and Xin Zhang*

State Key Laboratory of Chemical Resource Engineering, Beijing Advanced Innovation Center for Soft Matter Science and Engineering, Beijing University of Chemical Technology, Beijing 100029, P. R. China

Author Information

* Corresponding authors. Tel: +86-10-64412131; Fax: +86-10-64425385.

E-mail addresses: yangyusen@mail.buct.edu.cn (Y. Yang); zhangxin@mail.buct.edu.cn (X. Zhang).

■ Computational Details

DFT Calculation. All the calculations were carried out by the Vienna *Ab initio* Simulation Package (VASP5.4.1) software package.¹ The exchange-correlation interactions were modeled by the functional of Perdew, Burke and Ernzerhof (PBE) within the generalized gradient approximation (GGA),² and the core electrons are described with the projector augmented wave (PAW) method.^{3,4} The Grimme's DFT-D3 method was added to investigate the effect of van der Waals interaction.⁵ We calculated graphene lattice constant of 2.466 Å, which is slightly larger than the experimental value of 2.464 Å (Supplementary Table 1), and the margin of error is only 0.08%. The energy and force convergence criteria of the self-consistent iteration were set to 10^{-5} eV and 0.02 eV/Å, respectively. To ensure that energy calculations converge well for both k-points and plane wave energy cut off, the k-points and plane wave energy cut off were tested (Supplementary Fig. 1 and 2). We find that a Monkhorst-Pack k-point mesh of $3 \times 3 \times 1$ and a plane wave energy cut off with this grid size of 400 eV are sufficient to ensure less than 0.05 eV variation between calculations of *CO adsorption. Therefore, a cutoff energy of 400 eV for plane-wave basis sets and a $3 \times 3 \times 1$ Monkhorst-Pack K-point was sampled in the Brillouin zone for structure optimization. A $12 \times 12 \times 1$ denser k-point grid was used in the electronic structure calculation. For the *ab-initio* Molecular-Dynamics (AIMD) simulations, the system temperature was maintained at 500 K by using the Nose-Hoover thermostat⁶. The step length and time in AIMD simulations is 2 fs and 5 ps, respectively.

Model Construction. The DMSC models were built based on a 4×3 supercell of primitive graphene containing 48 C atoms (the calculated lattice parameters of structure: $a = 9.865$ Å, $b = 12.805$ Å) and added a 15 Å vacuum space to reduce the interaction between adjacent layers. By removing ten or twelve carbon atoms to create vacancies, and then introducing 6 N atoms and two metal atoms in the carbon vacancies

center, M₁-M₂-N₆-Gra structures with three different coordinated environments were obtained (the metal atoms close to the B-axis direction of the unit cell are defined as M₁, and the metal atoms away from the A-axis direction are defined as M₂). To further investigate whether there is an interaction between adsorbate and adsorbate in adjacent periods, we build three larger models with *p*(4 × 3), *p*(5 × 3) and *p*(6 × 4), and calculated the adsorption energy of *COOH and *CO.⁷ The optimized configurations and adsorption energies were shown in Table S2. We believe that the cell size of *p*(4 × 3) is large enough to avoid the adsorbate-adsorbate interactions in adjacent periods.

Energy calculation. The adsorption energies (*E*_{ads}) of reactants and products were calculated according to the Eq. (1).

$$\Delta E_{\text{ads}} = E_{\text{total}} - (E_{\text{gas}} + E^*) \quad (1)$$

where *E*_{total} indicates the total energy of the system with an attached adsorbate, *E*_{gas} indicates the energy of a gas phase adsorbate, and *E*^{*} is the energy of the surface.

The adsorption and reaction free energies were calculated at room temperature and 1 atmosphere by including the contribution of the zero-point energy (ZPE) and vibrational entropy. The Gibbs free energy of each reactant and intermediate were calculated as Eq. (2).

$$\Delta G = \Delta E_{\text{DFT}} + \Delta ZPE - T\Delta S + \Delta \int C_p dT \quad (2)$$

where *E*_{DFT} indicates the static electron energy of the system at 0 K. ΔZPE indicate zero-point energy correction of the system. *T* indicates the reaction temperature (298.15 K in this work). ΔS indicates the entropy change of adsorbate. *C*_p indicates the specific heat at constant pressure of adsorbate.

The process of reducing CO₂ to CO undergoes two electron transfers, including the following three steps:





The Gibbs free energy changes (ΔG) of the reaction are calculated by the computational hydrogen electrode model (CHE) proposed by Nørskov et al.⁸ as Eq. (3-5):

$$\Delta G_1 = G_{*\text{COOH}} - (G_{*\text{CO}_2} + G_* + \frac{1}{2}G_{\text{H}_2}) + \Delta G_U + \Delta G_{\text{pH}} \quad (3)$$

$$\Delta G_2 = G_{*\text{COOH}} + G_{*\text{H}_2\text{O}} - (G_{*\text{COOH}} + \frac{1}{2}G_{\text{H}_2}) + \Delta G_U + \Delta G_{\text{pH}} \quad (4)$$

$$\Delta G_3 = G_{*\text{CO}} + G_* - G_{*\text{CO}_2} + \Delta G_{\text{pH}} \quad (5)$$

$\Delta G_U = -eU$, where U is the applied electrode potential. $\Delta G_{\text{pH}} = k_B T \times \ln 10 \times \text{pH}$, where k_B is the Boltzmann constant, and pH value is set to 0. In addition, the solvation effects for $*\text{COOH}$ and $*\text{CO}$ are stabilized by -0.25 and -0.10 eV, respectively.^{9, 10} Due to the inaccurate description of CO molecules by the PBE functional, we added a correction of -0.51 eV for CO.¹¹

The limiting potential (U_L) of CO₂RR is defined as Eq. (6).

$$U_L = -\Delta G_{\max} / e = -\max(\Delta G_1, \Delta G_2, \Delta G_3) / e \quad (6)$$

The higher value of U_L , the higher the catalyst activity.

The selectivity descriptor (η) between CO₂RR and HER is defined using Eq. (7):

$$\eta = U_L(\text{CO}_2\text{RR}) - U_L(\text{HER}) \quad (7)$$

where $\eta > 0$ indicates CO₂RR is preferred over HER. Conversely, $\eta < 0$ indicates HER is preferred over CO₂RR.

Model evaluation. Two indexes that can describe prediction errors, the root-mean-square error (RMSE) and the coefficient of determination values (R^2 score), are applied to evaluate the performance of the ML models. The RMSE and R^2 score were calculated as Eq. (8) and Eq. (9), respectively.

$$RMSE = \sqrt{\frac{1}{n} \sum_{i=1}^n (y_i - \hat{y}_i)^2} \quad (8)$$

$$R^2 = 1 - \frac{\frac{1}{n} \sum_{i=1}^n (y_i - \hat{y}_i)^2}{\frac{1}{n} \sum_{i=1}^n (y_i - \bar{y})^2} \quad (9)$$

where \hat{y}_i indicates the ground truth, y_i indicates the prediction of the model and \bar{y} indicates the mean value. R^2 score ranges from 0 to 1, and the closer it is to 1, the better the prediction performance of the model is. RMSE represents the loss between the prediction and the ground truth. The loss is lower, the model performs better.

Supporting Tables

Table S1. Lattice parameters (in Å) of graphene as calculated with different functionals and comparison to experiment

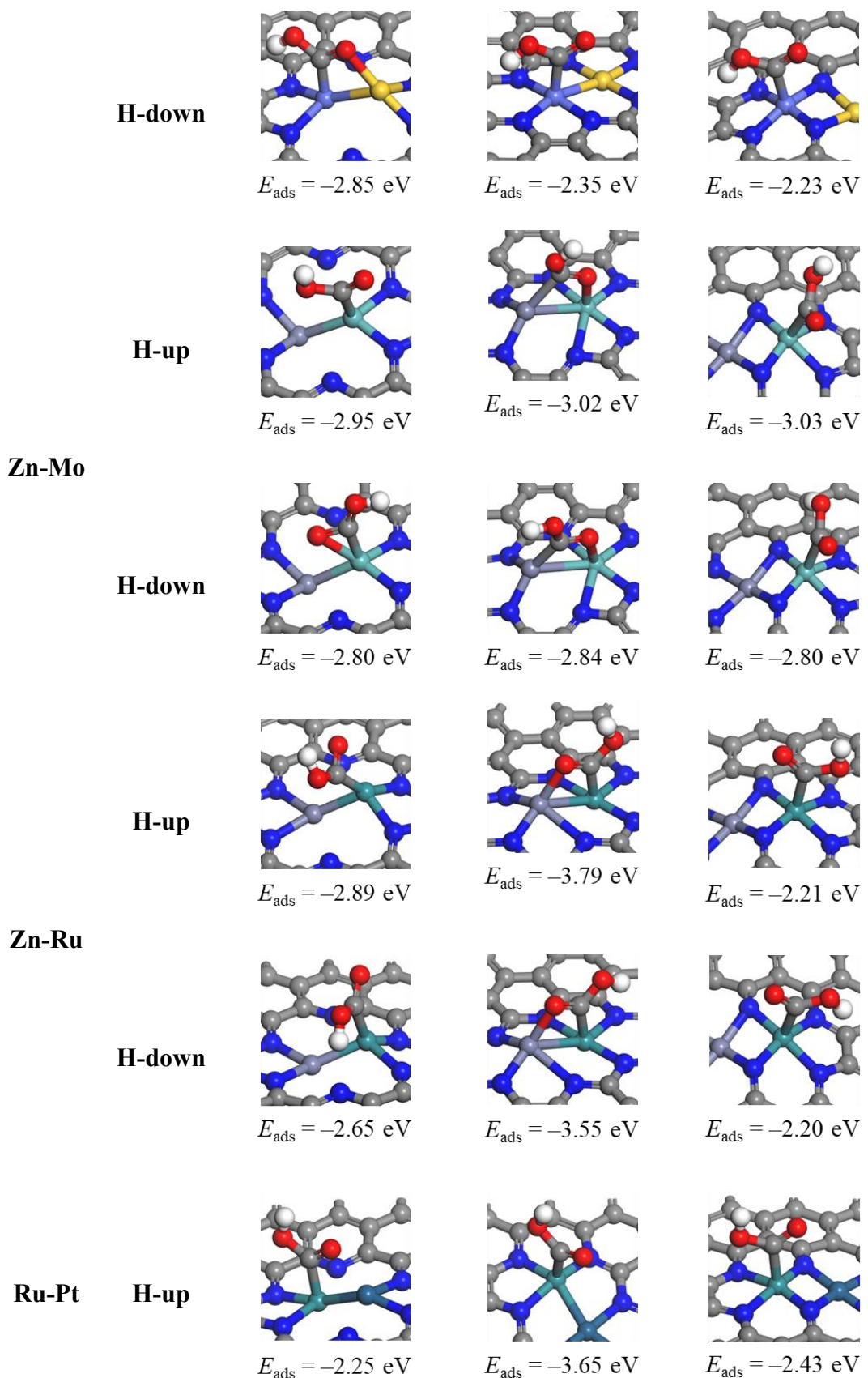
Method	Lattice constant
PBE-D3	$a = 2.466$
PBE	$a = 2.466$
PBEsol	$a = 2.464$
RPBE	$a = 2.468$
PW91	$a = 2.465$
Expt ¹²	$a = 2.464$

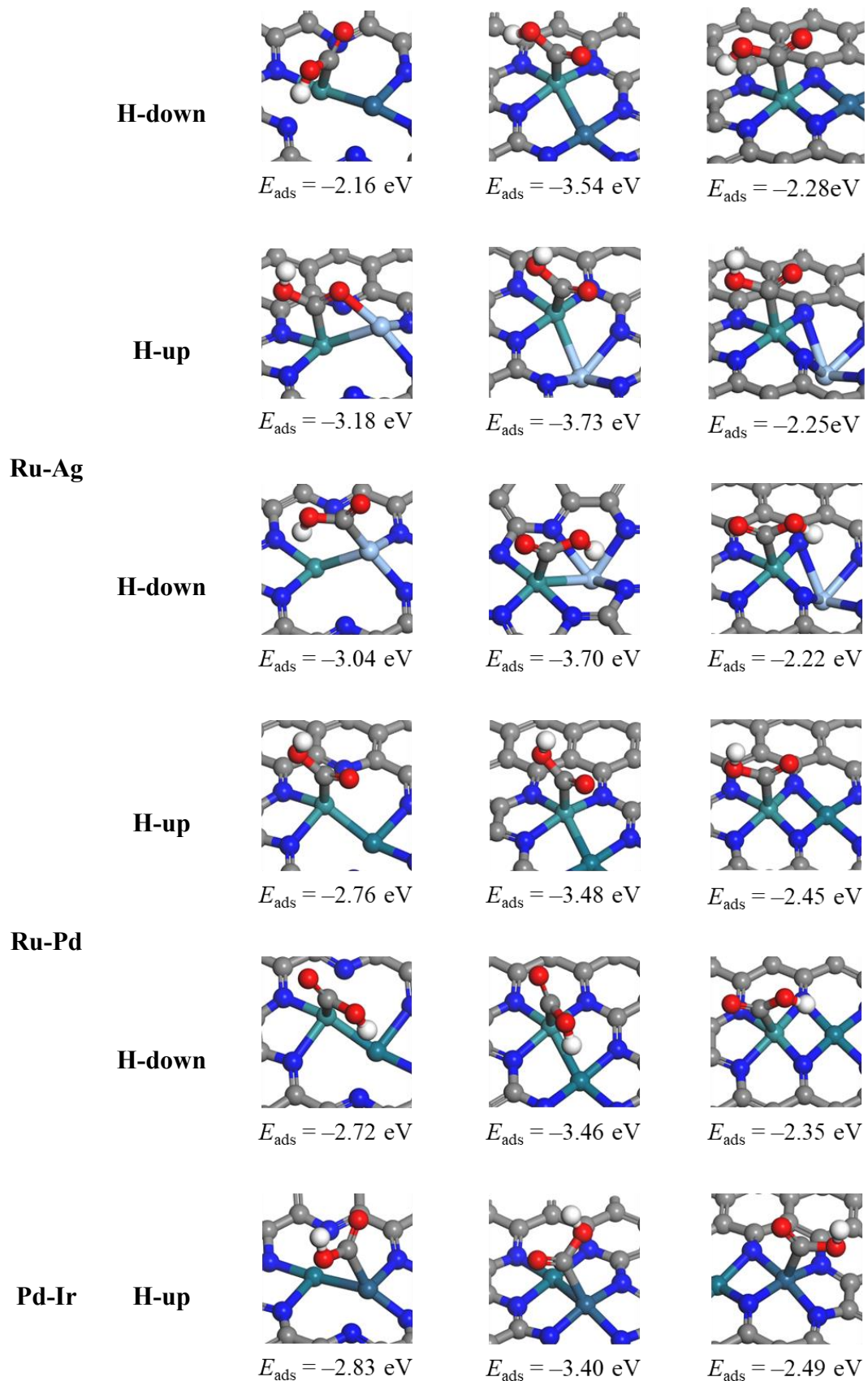
Table S2. The adsorption energies (E_{ads}) of $^{*}\text{COOH}$ and $^{*}\text{CO}$ on $p(4 \times 3)$, $p(5 \times 3)$, and $p(6 \times 4)$ supercells of Ni-Fe-N₆-Gra (Model 1, Model 2, Model 3) surfaces, respectively⁷. $E_{\text{ads}} = E_{\text{C}} - E_{M_1-M_2-N_6-\text{Gra}} - E_{\text{C}}$, where E_{C} and E^{*}_{C} represent the energies before and after the adsorption of C species on the M₁-M₂-N₆-Gra catalyst, respectively

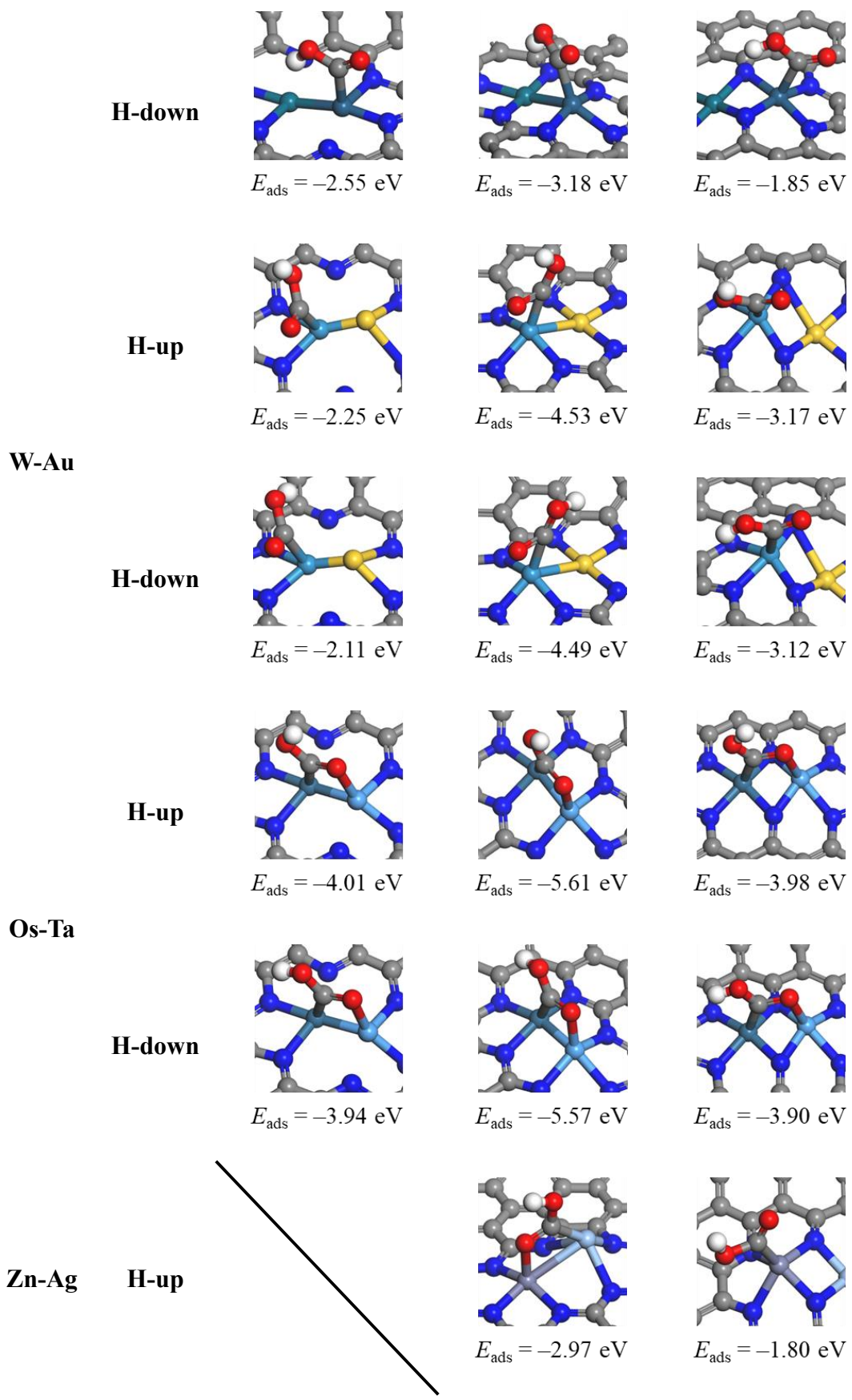
Supercell	Model 1		Model 2		Model 3	
	$^{*}\text{COOH}$	$^{*}\text{CO}$	$^{*}\text{COOH}$	$^{*}\text{CO}$	$^{*}\text{COOH}$	$^{*}\text{CO}$
4 × 3						
	$E_{\text{ads}} = -4.12 \text{ eV}$	$E_{\text{ads}} = -3.28 \text{ eV}$	$E_{\text{ads}} = -2.26 \text{ eV}$	$E_{\text{ads}} = -1.81 \text{ eV}$	$E_{\text{ads}} = -2.14 \text{ eV}$	$E_{\text{ads}} = -0.96 \text{ eV}$
5 × 3						
	$E_{\text{ads}} = -4.08 \text{ eV}$	$E_{\text{ads}} = -3.36 \text{ eV}$	$E_{\text{ads}} = -2.27 \text{ eV}$	$E_{\text{ads}} = -1.83 \text{ eV}$	$E_{\text{ads}} = -2.19 \text{ eV}$	$E_{\text{ads}} = -1.04 \text{ eV}$
6 × 4						
	$E_{\text{ads}} = -4.06 \text{ eV}$	$E_{\text{ads}} = -3.20 \text{ eV}$	$E_{\text{ads}} = -2.28 \text{ eV}$	$E_{\text{ads}} = -1.86 \text{ eV}$	$E_{\text{ads}} = -2.09 \text{ eV}$	$E_{\text{ads}} = -1.01 \text{ eV}$

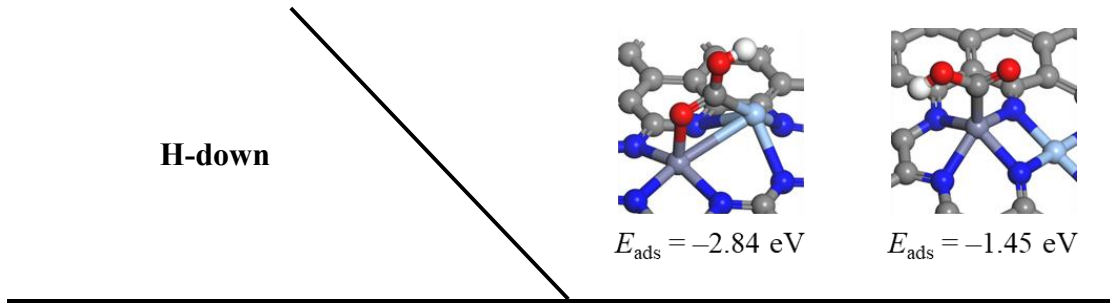
Table S3. Optimized geometries and adsorption energies (E_{ads}) of adsorbed cis-COOH (H-up) and trans-COOH (H-down) on M1-M2-N₆-Gra

*COOH	Model 1	Model 2	Model 3
H-up			
	$E_{\text{ads}} = -2.71 \text{ eV}$	$E_{\text{ads}} = -2.34 \text{ eV}$	$E_{\text{ads}} = -2.31 \text{ eV}$
Fe-Pd			
H-down			
	$E_{\text{ads}} = -2.62 \text{ eV}$	$E_{\text{ads}} = -2.12 \text{ eV}$	$E_{\text{ads}} = -2.14 \text{ eV}$
H-up			
	$E_{\text{ads}} = -2.58 \text{ eV}$	$E_{\text{ads}} = -2.68 \text{ eV}$	$E_{\text{ads}} = -2.10 \text{ eV}$
Co-Pt			
H-down			
	$E_{\text{ads}} = -2.56 \text{ eV}$	$E_{\text{ads}} = -2.57 \text{ eV}$	$E_{\text{ads}} = -2.03 \text{ eV}$
Co-Au	H-up		
		$E_{\text{ads}} = -2.92 \text{ eV}$	$E_{\text{ads}} = -2.42 \text{ eV}$
			$E_{\text{ads}} = -2.35 \text{ eV}$









We examine the adsorption configurations and adsorption energies of trans-COOH (H-down) on M1-M2-N₆-Gra. The calculation results show that the adsorption energies of cis-COOH (H-up) are more negative than that of tran-COOH (H-down) indicating that the cis-COOH adsorption configuration is more stable.

Table S4. The computational limiting potentials and potential determining steps for CO production on M₁-M₂-N₆-Gra at 0 V vs RHE

M ₁ -M ₂ -N ₆ -Gra	Model 1		Model 2		Model 3	
	U _L (V)	PDS	U _L (V)	PDS	U _L (V)	PDS
Fe-Pd	-0.95	*CO → CO	-0.84	*CO → CO	-0.21	*CO → CO
Zn-Mo	-1.25	*CO → CO	-1.6	*CO → CO	-1.30	*COOH → *CO
Zn-Ru	-1.71	*CO → CO	-1.65	*CO → CO	-0.35	*CO → CO
Zn-Ag	—	—	-0.84	*COOH → *CO	-0.67	CO ₂ → *COOH
Ru-Ag	-1.46	*CO → CO	-1.82	*CO → CO	-0.42	*COOH → *CO
Ru-Pd	-1.47	*CO → CO	-2.06	*CO → CO	-0.12	CO ₂ → *COOH
Co-Au	-1.62	*CO → CO	-0.61	*CO → CO	-0.17	CO ₂ → *COOH
Co-Pt	-1.20	*CO → CO	-1.15	*CO → CO	-0.41	CO ₂ → *COOH
Pd-Ir	-1.37	*CO → CO	-1.94	*CO → CO	-0.34	*CO → CO
Ru-Pt	-1.06	*CO → CO	-2.06	*CO → CO	-0.11	*CO → CO
Os-Ta	-0.97	*COOH → *CO	-2.58	*CO → CO	-0.97	*CO → CO
W-Au	-0.83	*CO → CO	-2.12	*CO → CO	-1.36	*CO → CO

Table S5. The adsorption energy of *COOH and *CO over DMSCs obtained from our previous work⁷

	Model1		Model2		Model2	
	$E_{\text{ads}}(\text{*COOH})$	$E_{\text{ads}}(\text{*CO})$	$E_{\text{ads}}(\text{*COOH})$	$E_{\text{ads}}(\text{*CO})$	$E_{\text{ads}}(\text{*COOH})$	$E_{\text{ads}}(\text{*CO})$
Ni-Mn	-3.65	-2.49	-2.17	-1.34	-2.18	-1.11
Ni-Fe	-4.12	-3.28	-2.26	-1.81	-2.14	-0.96
Ni-Co	-2.98	-2.66	-2.58	-1.96	-1.96	-0.58
Ni-Ni	-2.72	-2.61	-1.90	-1.00	-1.01	-0.09
Ni-Cu	-2.74	-2.40	-1.77	-0.89	-1.01	-0.07
Ni-Zn	-3.20	-2.69	-2.42	-1.49	-1.40	-0.27
Fe-Mn	-3.69	-2.53	-3.18	-2.40	-2.25	-0.80
Fe-Fe	-3.33	-2.41	-2.83	-2.17	-2.04	-0.64
Fe-Co	-4.06	-3.25	-2.45	-1.89	-2.09	-0.64
Fe-Cu	-3.13	-2.39	-2.47	-1.76	-2.28	-1.18
Fe-Zn	-2.97	-2.27	-3.08	-2.28	-2.35	-1.17
Cu-Mn	-4.86	-3.46	-2.34	-1.42	-2.25	-1.20
Cu-Co	-3.07	-2.59	-2.38	-1.56	-2.09	-0.76
Cu-Cu	-2.82	-2.36	-1.37	-0.75	-0.65	-0.08
Cu-Zn	-3.12	-1.60	-2.13	-0.85	-1.63	-0.21
Mn-Mn	-3.32	-2.23	-3.09	-2.34	-2.41	-0.65
Mn-Co	-3.65	-2.66	-3.09	-2.16	-2.16	-1.15
Mn-Zn	-3.75	-2.93	-3.13	-2.00	-2.39	-1.18
Co-Co	-3.35	-2.75	-2.45	-2.30	-1.61	-0.11
Co-Zn	-3.04	-2.61	-2.97	-2.14	-2.29	-0.96
Zn-Zn	-1.68	-0.38	-3.03	-0.40	-1.48	-0.34

Table S6. Complete feature space of individual and composite feature

Features	Description
R1	Atomic Radius of M ₁
R2	Atomic Radius of M ₂
n1	d Electron Numbers of M ₁
n2	d Electron Numbers of M ₂
G1	Group of M ₁
G2	Group of M ₂
E1	Pauling Electronegativity of M ₁
E2	Pauling Electronegativity of M ₂
δ1	1 st Ionization Energy of M ₁
δ2	1 st Ionization Energy of M ₂
σ1	Electron Affinity of M ₁
σ2	Electron Affinity of M ₂
R+	Addition between Atomic Radius
d+	Addition between d Electron Numbers
G+	Addition between Group
E+	Addition between Pauling Electronegativity
δ+	Addition between 1 st Ionization Energy
σ+	Addition between Electron Affinity
R-	Absolute Value of Difference between Atomic Radius
d-	Absolute Value of Difference between d Electron Numbers
G-	Absolute Value of Difference between Group
E-	Absolute Value of Difference between Pauling Electronegativity
δ-	Absolute Value of Difference between 1 st Ionization Energy
σ-	Absolute Value of Difference between Electron Affinity
ω	Coordination Number
e1	the number of charge gains/losses for M ₁
e2	the number of charge gains/losses for M ₂

e^+	Addition between the number of charge gains/losses
e^-	Absolute Value of Difference between the number of charge gains/losses
d	the distance between M_1 and M_2

Table S7. The specific workflow for screening descriptors

	1st	2nd	3rd	4th	5th	6th
Number of Descriptors	25	21	16	13	12	10
RMSE (eV)	0.15	0.15	0.15	0.15	0.15	0.17
R²	0.91	0.92	0.92	0.92	0.92	0.90
	<i>R</i> 1, <i>R</i> 2, <i>R</i> +, <i>R</i> -, <i>n</i> 1, <i>n</i> 2, <i>n</i> +, <i>n</i> -,	<i>R</i> 1, <i>R</i> 2, <i>R</i> +, <i>R</i> -, <i>n</i> +,	<i>R</i> +, <i>R</i> -, <i>n</i> +,	<i>R</i> +, <i>R</i> -, <i>G</i> -,	<i>R</i> +, <i>G</i> 1, <i>G</i> 2,	<i>R</i> +, <i>G</i> 1, <i>G</i> 2,
	<i>G</i> 1, <i>G</i> 2, <i>G</i> +, <i>G</i> -,	<i>G</i> 1, <i>G</i> 2, <i>G</i> -, <i>E</i> 1, <i>E</i> 2, <i>E</i> +, <i>E</i> -,	<i>G</i> 1, <i>G</i> 2, <i>G</i> -, <i>E</i> 1, <i>E</i> 2, <i>E</i> -,	<i>G</i> 1, <i>G</i> 2, <i>G</i> -,	<i>G</i> 1, <i>G</i> 2, <i>G</i> -,	<i>G</i> 1, <i>G</i> 2, <i>G</i> -,
	<i>E</i> 1, <i>E</i> 2, <i>E</i> +, <i>E</i> -, <i>δ</i> 1, <i>δ</i> 2, <i>δ</i> +, <i>δ</i> -,	<i>δ</i> 1, <i>δ</i> 2, <i>σ</i> 1, <i>σ</i> 2, <i>σ</i> +, <i>σ</i> -,	<i>δ</i> 1, <i>δ</i> 2, <i>σ</i> +, <i>σ</i> -, <i>ω</i>	<i>E</i> 1, <i>E</i> 2, <i>E</i> -, <i>δ</i> +, <i>δ</i> -,	<i>E</i> 1, <i>E</i> 2, <i>E</i> -, <i>δ</i> +, <i>δ</i> -,	<i>E</i> 1, <i>E</i> 2, <i>E</i> -, <i>σ</i> +, <i>σ</i> -, <i>ω</i>
	<i>ω</i>					

Table S8. The atomic parameters of the selected element

Element	Radius (pm)	d electron count	Group	Electronegativity	1 st Ionization Energy (eV)	Electron Affinity (eV)
Sc	184	1	3	1.36	6.562	0.188
Ti	176	2	4	1.54	6.828	0.079
V	171	3	5	1.63	6.746	0.524
Cr	166	5	6	1.66	6.767	0.666
Mn	161	5	7	1.55	7.434	0.000
Fe	156	6	8	1.83	7.903	0.163
Co	152	7	9	1.88	7.881	0.660
Ni	149	8	10	1.90	7.640	1.160
Cu	145	10	11	1.90	7.727	1.227
Zn	142	10	12	1.65	9.394	0.000
Y	212	1	3	1.22	6.220	0.307
Zr	206	2	4	1.33	6.634	0.426
Nb	198	4	5	1.60	6.759	0.892
Mo	190	5	6	2.16	7.092	0.745
Tc	183	5	7	1.90	7.280	0.550
Ru	178	7	8	2.20	7.361	1.050
Rh	173	8	9	2.28	7.459	1.137
Pd	169	8	10	2.20	8.337	0.557
Ag	165	10	11	1.93	7.576	1.302
Cd	161	10	12	1.69	8.994	0.000
Hf	208	2	4	1.30	6.825	0.000
Ta	200	3	5	1.50	7.890	0.320
W	193	4	6	2.36	7.980	0.815
Re	188	5	7	1.90	7.880	0.150
Os	185	6	8	2.20	8.710	1.100
Ir	180	7	9	2.20	9.120	1.570
Pt	177	9	10	2.28	9.020	2.128
Au	174	10	11	2.54	9.225	2.309

Table S9. 1st Machine learning data set with selected features for $U_L(V)$ of CO production

M ₁ -M ₂ -N ₆ -Gra	G1	E1	G2	E2	R+	δ+	σ+	G-	E-	δ-	σ-	ω	$U_L(V)$
Ni-Mn	10	1.90	7	1.55	310	15.074	1.160	3	0.35	0.206	1.160	2	-1.55
Ni-Fe	10	1.90	8	1.83	305	15.543	1.323	2	0.07	0.263	0.997	2	-2.34
Ni-Co	10	1.90	9	1.88	301	15.521	1.820	1	0.02	0.241	0.500	2	-1.72
Ni-Ni	10	1.90	10	1.90	298	15.280	2.320	0	0.00	0.000	0.000	2	-1.64
Ni-Cu	10	1.90	11	1.90	294	15.367	2.387	1	0.00	0.087	0.067	2	-1.45
Ni-Zn	10	1.90	12	1.65	291	17.034	1.160	2	0.25	1.754	1.160	2	-1.72
Fe-Mn	8	1.83	7	1.55	317	15.337	0.163	1	0.28	0.469	0.163	2	-1.61
Fe-Fe	8	1.83	8	1.83	312	15.806	0.326	0	0.00	0.000	0.000	2	-1.49
Fe-Co	8	1.83	9	1.88	308	15.783	0.823	1	0.05	0.023	0.497	2	-2.31
Fe-Cu	8	1.83	11	1.90	301	15.630	1.390	3	0.07	0.176	1.064	2	-1.46
Fe-Zn	8	1.83	12	1.65	298	17.297	0.163	4	0.18	1.491	0.163	2	-1.34
Cu-Mn	11	1.90	7	1.55	306	15.161	1.227	4	0.35	0.293	1.227	2	-2.49
Cu-Co	11	1.90	9	1.88	297	15.608	1.887	2	0.02	0.154	0.567	2	-1.66
Cu-Cu	11	1.90	11	1.90	290	15.454	2.454	0	0.00	0.000	0.000	2	-1.42
Cu-Zn	11	1.90	12	1.65	287	17.121	1.227	1	0.25	1.667	1.227	2	-0.64
Mn-Mn	7	1.55	7	1.55	322	14.868	0.000	0	0.00	0.000	0.000	2	-1.31
Mn-Co	7	1.55	9	1.88	313	15.315	0.660	2	0.33	0.447	0.660	2	-1.73
Mn-Zn	7	1.55	12	1.65	303	16.828	0.000	5	0.10	1.960	0.000	2	-1.98
Co-Co	9	1.88	9	1.88	304	15.762	1.320	0	0.00	0.000	0.000	2	-1.81
Co-Zn	9	1.88	12	1.65	294	17.275	0.660	3	0.23	1.513	0.660	2	-1.66
Zn-Zn	12	1.65	12	1.65	284	18.788	0.000	0	0.00	0.000	0.000	2	-0.83
Fe-Pd	8	1.83	10	2.20	325	16.240	0.720	2	0.37	0.434	0.394	2	-0.95
Zn-Mo	12	1.65	6	2.16	332	16.486	0.745	6	0.51	2.302	0.745	2	-1.25
Zn-Ru	12	1.65	8	2.20	320	16.755	1.050	4	0.55	2.033	1.050	2	-1.71
Ru-Ag	8	2.20	11	1.93	343	14.937	2.352	3	0.27	0.215	0.252	2	-1.46
Ru-Pd	8	2.20	10	2.20	347	15.698	1.607	2	0.00	0.976	0.493	2	-1.47
Co-Au	9	1.88	11	2.54	326	17.106	2.969	2	0.66	1.344	1.649	2	-1.62
Co-Pt	9	1.88	10	2.28	329	16.901	2.788	1	0.40	1.139	1.468	2	-1.20
Pd-Ir	10	2.20	9	2.20	349	17.457	2.127	1	0.00	0.783	1.013	2	-1.37
Ru-Pt	8	2.20	10	2.28	355	16.381	3.178	2	0.08	1.659	1.078	2	-1.06
Os-Ta	8	2.20	5	1.50	385	16.600	1.420	3	0.70	0.820	0.780	2	-0.97
W-Au	6	2.36	11	2.54	367	17.205	3.124	5	0.18	1.245	1.494	2	-0.83
Ni-Mn	10	1.90	7	1.55	310	15.074	1.160	3	0.35	0.206	1.160	3	-0.38
Ni-Fe	10	1.90	8	1.83	305	15.543	1.323	2	0.07	0.263	0.997	3	-0.84
Ni-Co	10	1.90	9	1.88	301	15.521	1.820	1	0.02	0.241	0.500	3	-1.01
Ni-Ni	10	1.90	10	1.90	298	15.280	2.320	0	0.00	0.000	0.000	3	-0.63
Ni-Cu	10	1.90	11	1.90	294	15.367	2.387	1	0.00	0.087	0.067	3	-0.74
Ni-Zn	10	1.90	12	1.65	291	17.034	1.160	2	0.25	1.754	1.160	3	-0.58
Fe-Mn	8	1.83	7	1.55	317	15.337	0.163	1	0.28	0.469	0.163	3	-1.45
Fe-Fe	8	1.83	8	1.83	312	15.806	0.326	0	0.00	0.000	0.000	3	-1.21
Fe-Co	8	1.83	9	1.88	308	15.783	0.823	1	0.05	0.023	0.497	3	-0.93

Fe-Cu	8	1.83	11	1.90	301	15.630	1.390	3	0.07	0.176	1.064	3	-0.79
Fe-Zn	8	1.83	12	1.65	298	17.297	0.163	4	0.18	1.491	0.163	3	-1.33
Cu-Mn	11	1.90	7	1.55	306	15.161	1.227	4	0.35	0.293	1.227	3	-0.50
Cu-Co	11	1.9	9	1.88	297	15.608	1.887	2	0.02	0.154	0.567	3	-0.63
Cu-Cu	11	1.90	11	1.90	290	15.454	2.454	0	0.00	0.000	0.000	3	-1.10
Cu-Zn	11	1.90	12	1.65	287	17.121	1.227	1	0.25	1.667	1.227	3	-0.41
Mn-Mn	7	1.55	7	1.55	322	14.868	0.000	0	0.00	0.000	0.000	3	-1.44
Mn-Co	7	1.55	9	1.88	313	15.315	0.660	2	0.33	0.447	0.660	3	-1.21
Mn-Zn	7	1.55	12	1.65	303	16.828	0.000	5	0.10	1.960	0.000	3	-1.07
Co-Co	9	1.88	9	1.88	304	15.762	1.320	0	0.00	0.000	0.000	3	-1.34
Co-Zn	9	1.88	12	1.65	294	17.275	0.660	3	0.23	1.513	0.660	3	-1.19
Zn-Zn	12	1.65	12	1.65	284	18.788	0.000	0	0.00	0.000	0.000	3	-1.08
Fe-Pd	8	1.83	10	2.20	325	16.240	0.72	2	0.37	0.434	0.394	3	-0.84
Zn-Mo	12	1.65	6	2.16	332	16.486	0.745	6	0.51	2.302	0.745	3	-1.60
Zn-Ru	12	1.65	8	2.20	320	16.755	1.050	4	0.55	2.033	1.050	3	-1.65
Zn-Ag	12	1.65	11	1.93	307	16.970	1.302	1	0.28	1.818	1.302	3	-0.84
Ru-Ag	8	2.20	11	1.93	343	14.937	2.352	3	0.27	0.215	0.252	3	-1.82
Ru-Pd	8	2.20	10	2.20	347	15.698	1.607	2	0.00	0.976	0.493	3	-2.06
Co-Au	9	1.88	11	2.54	326	17.106	2.969	2	0.66	1.344	1.649	3	-0.61
Co-Pt	9	1.88	10	2.28	329	16.901	2.788	1	0.40	1.139	1.468	3	-1.15
Pd-Ir	10	2.20	9	2.20	349	17.457	2.127	1	0.00	0.783	1.013	3	-1.94
Ru-Pt	8	2.20	10	2.28	355	16.381	3.178	2	0.08	1.659	1.078	3	-2.06
Os-Ta	8	2.20	5	1.50	385	16.600	1.420	3	0.70	0.820	0.780	3	-2.58
W-Au	6	2.36	11	2.54	367	17.205	3.124	5	0.18	1.245	1.494	3	-2.12
Ni-Mn	10	1.90	7	1.55	310	15.074	1.160	3	0.35	0.206	1.16	4	-0.33
Ni-Fe	10	1.90	8	1.83	305	15.543	1.323	2	0.07	0.263	0.997	4	-0.42
Ni-Co	10	1.90	9	1.88	301	15.521	1.820	1	0.02	0.241	0.500	4	-0.55
Ni-Ni	10	1.90	10	1.90	298	15.280	2.320	0	0.00	0.000	0.000	4	-1.49
Ni-Cu	10	1.90	11	1.90	294	15.367	2.387	1	0.00	0.087	0.067	4	-1.51
Ni-Zn	10	1.90	12	1.65	291	17.034	1.160	2	0.25	1.754	1.160	4	-1.08
Fe-Mn	8	1.83	7	1.55	317	15.337	0.163	1	0.28	0.469	0.163	4	-0.27
Fe-Fe	8	1.83	8	1.83	312	15.806	0.326	0	0.00	0.000	0.000	4	-0.49
Fe-Co	8	1.83	9	1.88	308	15.783	0.823	1	0.05	0.023	0.497	4	-0.44
Fe-Cu	8	1.83	11	1.90	301	15.630	1.390	3	0.07	0.176	1.064	4	-0.24
Fe-Zn	8	1.83	12	1.65	298	17.297	0.163	4	0.18	1.491	0.163	4	-0.23
Cu-Mn	11	1.90	7	1.55	306	15.161	1.227	4	0.35	0.293	1.227	4	-0.27
Cu-Co	11	1.90	9	1.88	297	15.608	1.887	2	0.02	0.154	0.567	4	-0.43
Cu-Cu	11	1.90	11	1.90	290	15.454	2.454	0	0.00	0.000	0.000	4	-1.84
Cu-Zn	11	1.90	12	1.65	287	17.121	1.227	1	0.25	1.667	1.227	4	-0.88
Mn-Mn	7	1.55	7	1.55	322	14.868	0.000	0	0.00	0.000	0.000	4	-0.32
Mn-Co	7	1.55	9	1.88	313	15.315	0.660	2	0.33	0.447	0.660	4	-0.35
Mn-Zn	7	1.55	12	1.65	303	16.828	0.000	5	0.10	1.960	0.000	4	-0.25
Co-Co	9	1.88	9	1.88	304	15.762	1.320	0	0.00	0.000	0.000	4	-0.90
Co-Zn	9	1.88	12	1.65	294	17.275	0.660	3	0.23	1.513	0.660	4	-0.22

Zn-Zn	12	1.65	12	1.65	284	18.788	0.000	0	0.00	0.000	0.000	4	-1.02
Fe-Pd	8	1.83	10	2.20	325	16.240	0.720	2	0.37	0.434	0.394	4	-0.21
Zn-Mo	12	1.65	6	2.16	332	16.486	0.745	6	0.51	2.302	0.745	4	-1.30
Zn-Ru	12	1.65	8	2.20	320	16.755	1.050	4	0.55	2.033	1.05	4	-0.35
Zn-Ag	12	2.20	11	1.93	307	16.970	1.302	1	0.27	1.818	1.302	4	-0.67
Ru-Ag	8	2.20	11	1.93	343	14.937	2.352	3	0.27	0.215	0.252	4	-0.42
Ru-Pd	8	2.20	10	2.20	347	15.698	1.607	2	0.00	0.976	0.493	4	-0.12
Co-Au	9	1.88	11	2.54	326	17.106	2.969	2	0.66	1.344	1.649	4	-0.17
Co-Pt	9	1.88	10	2.28	329	16.901	2.788	1	0.40	1.139	1.468	4	-0.41
Pd-Ir	10	2.20	9	2.20	349	17.457	2.127	1	0.00	0.783	1.013	4	-0.34
Ru-Pt	8	2.20	10	2.28	355	16.381	3.178	2	0.08	1.659	1.078	4	-0.11
Os-Ta	8	2.20	5	1.50	385	16.600	1.420	3	0.70	0.820	0.780	4	-0.97
W-Au	6	2.36	11	2.54	367	17.205	3.124	5	0.18	1.245	1.494	4	-1.36

Table S10. The 5 times the 5-fold cross validation for the 1st round of ML

	Fold 1	Fold 2	Fold 3	Fold 4	Fold 5	Average
1	0.15	0.15	0.15	0.15	0.15	0.15
2	0.15	0.15	0.15	0.15	0.15	0.15
3	0.15	0.15	0.15	0.15	0.15	0.15
4	0.15	0.15	0.15	0.16	0.16	0.15
5	0.15	0.15	0.15	0.16	0.16	0.15
Average	0.15	0.15	0.15	0.15	0.15	0.15

Table S11. 2nd Machine learning data set with extra selected features for $U_L(V)$ of CO production

M ₁ -M ₂ -N ₆ -Gra	e1	e2	e+	e-	d	ω
Ni-Mn	-0.39	-1.00	-1.39	0.61	2.25	2
Ni-Fe	-0.50	-0.70	-1.20	0.20	2.22	2
Ni-Co	-0.50	-0.58	-1.08	0.08	2.25	2
Ni-Ni	-0.59	-0.59	-1.18	0.00	2.34	2
Ni-Cu	-0.59	-0.55	-1.14	0.04	2.30	2
Ni-Zn	-0.55	-0.65	-1.20	0.10	2.29	2
Fe-Mn	-0.61	-0.90	-1.51	0.29	2.13	2
Fe-Fe	-0.78	-0.78	-1.56	0.00	2.28	2
Fe-Co	-0.84	-0.44	-1.28	0.40	2.11	2
Fe-Cu	-0.72	-0.49	-1.21	0.23	2.29	2
Fe-Zn	-0.73	-0.63	-1.36	0.10	2.30	2
Cu-Mn	-0.22	-0.99	-1.21	0.77	2.23	2
Cu-Co	-0.51	-0.67	-1.18	0.16	2.29	2
Cu-Cu	-0.57	-0.56	-1.13	0.01	2.33	2
Cu-Zn	-0.40	-0.68	-1.08	0.28	2.24	2
Mn-Mn	-0.84	-0.86	-1.70	0.01	2.22	2
Mn-Co	-0.98	-0.49	-1.47	0.49	2.18	2
Mn-Zn	-1.09	-0.31	-1.40	0.78	2.32	2
Co-Co	-0.58	-0.60	-1.18	0.02	2.24	2
Co-Zn	-0.56	-0.77	-1.33	0.21	2.31	2
Zn-Zn	-0.67	-0.60	-1.27	0.07	2.22	2
Fe-Pd	-0.95	-0.30	-1.25	0.65	2.26	2
Zn-Mo	-0.57	-1.02	-1.59	0.45	2.44	2
Zn-Ru	-0.78	-0.51	-1.29	0.27	2.37	2
Ru-Ag	-0.63	-0.36	-0.99	0.27	2.59	2
Ru-Pd	-0.62	-0.44	-1.06	0.18	2.39	2
Co-Au	-0.85	-0.09	-0.94	0.75	2.43	2
Co-Pt	-0.69	-0.32	-1.01	0.37	2.34	2
Pd-Ir	-0.43	-0.51	-0.94	0.08	2.41	2
Ru-Pt	-0.64	-0.41	-1.05	0.23	2.42	2
Os-Ta	-0.34	-1.37	-1.71	1.03	2.17	2
W-Au	-1.43	0.37	-1.06	1.79	2.50	2
Ni-Mn	-0.52	-1.08	-1.60	0.56	2.26	3
Ni-Fe	-0.58	-0.93	-1.51	0.35	2.27	3
Ni-Co	-0.56	-0.71	-1.27	0.15	2.31	3
Ni-Ni	-0.61	-0.58	-1.19	0.03	2.34	3
Ni-Cu	-0.69	-0.71	-1.40	0.02	2.38	3
Ni-Zn	-0.56	-0.99	-1.55	0.43	2.43	3
Fe-Mn	-0.75	-1.01	-1.76	0.26	2.34	3
Fe-Fe	-0.87	-0.86	-1.73	0.01	2.21	3
Fe-Co	-0.89	-0.62	-1.51	0.27	2.17	3
Fe-Cu	-0.88	-0.66	-1.54	0.22	2.40	3

Fe-Zn	-0.81	-0.99	-1.80	0.18	2.43	3
Cu-Mn	-0.59	-1.10	-1.69	0.51	2.40	3
Cu-Co	-0.69	-0.64	-1.33	0.05	2.40	3
Cu-Cu	-0.72	-0.72	-1.44	0.00	2.38	3
Cu-Zn	-0.60	-1.00	-1.60	0.40	2.39	3
Mn-Mn	-0.94	-0.91	-1.85	0.03	2.37	3
Mn-Co	-1.00	-0.52	-1.52	0.48	2.22	3
Mn-Zn	-1.07	-0.93	-2.00	0.14	2.49	3
Co-Co	-0.64	-0.66	-1.30	0.02	2.23	3
Co-Zn	-0.64	-0.95	-1.59	0.31	2.41	3
Zn-Zn	-0.99	-0.99	-1.98	0.00	2.55	3
Fe-Pd	-0.95	-0.40	-1.35	0.55	2.32	3
Zn-Mo	-0.74	-1.04	-1.78	0.30	2.39	3
Zn-Ru	-0.96	-0.59	-1.55	0.37	2.39	3
Zn-Ag	-1.00	-0.52	-1.52	0.48	2.38	3
Ru-Ag	-0.74	-0.56	-1.30	0.18	2.44	3
Ru-Pd	-0.71	-0.46	-1.17	0.25	2.36	3
Co-Au	-0.72	-0.52	-1.24	0.20	2.37	3
Co-Pt	-0.76	-0.39	-1.15	0.37	2.33	3
Pd-Ir	-0.52	-0.56	-1.08	0.03	2.41	3
Ru-Pt	-0.81	-0.41	-1.22	0.41	2.37	3
Os-Ta	-0.45	-1.52	-1.97	1.07	2.15	3
W-Au	-1.33	-0.42	-1.75	0.91	2.46	3
Ni-Mn	-0.82	-1.25	-2.07	0.43	2.46	4
Ni-Fe	-0.85	-1.11	-1.96	0.26	2.44	4
Ni-Co	-0.87	-0.89	-1.76	0.02	2.42	4
Ni-Ni	-0.87	-0.85	-1.72	0.02	2.58	4
Ni-Cu	-0.84	-0.95	-1.79	0.11	2.55	4
Ni-Zn	-0.83	-1.16	-1.99	0.33	2.55	4
Fe-Mn	-0.87	-1.21	-2.08	0.34	2.24	4
Fe-Fe	-1.00	-0.99	-1.99	0.01	2.22	4
Fe-Co	-0.90	-0.86	-1.76	0.04	2.25	4
Fe-Cu	-1.06	-0.91	-1.97	0.15	2.45	4
Fe-Zn	-1.05	-1.14	-2.19	0.09	2.45	4
Cu-Mn	-0.87	-1.22	-2.09	0.35	2.33	4
Cu-Co	-0.93	-0.90	-1.83	0.03	2.43	4
Cu-Cu	-0.91	-0.92	-1.83	0.01	2.58	4
Cu-Zn	-0.93	-1.16	-2.09	0.23	2.63	4
Mn-Mn	-1.12	-1.21	-2.33	0.09	2.27	4
Mn-Co	-1.21	-0.83	-2.04	0.38	2.26	4
Mn-Zn	-1.28	-1.14	-2.42	0.14	2.51	4
Co-Co	-0.76	-0.91	-1.67	0.15	2.26	4
Co-Zn	-0.89	-1.14	-2.03	0.25	2.47	4
Zn-Zn	-1.13	-1.13	-2.26	0.00	2.55	4

Fe-Pd	-1.14	-0.70	-1.84	0.44	2.48	4
Zn-Mo	-1.10	-1.39	-2.49	0.29	2.49	4
Zn-Ru	-1.10	-0.91	-2.01	0.19	2.42	4
Zn-Ag	-1.16	-0.84	-2.00	0.32	2.63	4
Ru-Ag	-1.02	-0.49	-1.51	0.53	2.73	4
Ru-Pd	-0.90	-0.69	-1.59	0.21	2.40	4
Co-Au	-0.82	-0.96	-1.78	0.14	2.65	4
Co-Pt	-0.93	-0.85	-1.78	0.08	2.48	4
Pd-Ir	-0.76	-0.89	-1.65	0.13	2.45	4
Ru-Pt	-0.90	-0.84	-1.74	0.06	2.40	4
Os-Ta	-0.82	-1.72	-2.54	0.90	2.42	4
W-Au	-1.61	-0.53	-2.14	1.08	2.55	4

Table S12. The 5 times the 5-fold cross validation for the 2nd round of ML

	Fold 1	Fold 2	Fold 3	Fold 4	Fold 5	Average
1	0.08	0.08	0.08	0.08	0.08	0.08
2	0.09	0.09	0.09	0.08	0.08	0.08
3	0.09	0.09	0.09	0.08	0.08	0.08
4	0.09	0.08	0.08	0.08	0.08	0.08
5	0.08	0.08	0.08	0.08	0.08	0.08
Average	0.08	0.08	0.08	0.08	0.08	0.08

Table S13. The data of CO₂RR filtered from the 1st ML for the 2nd ML prediction

M ₁ -M ₂ -N ₆ -Gra	<i>U_L(V)</i> of 1 st ML	<i>U_L(V)</i> of 2 nd ML
Fe-Rh	-0.24	-0.29
Mn-Os	-0.33	-0.23
Mn-Pd	-0.27	-0.24
Mn-Ru	-0.33	-0.28
Mn-Ir	-0.28	-0.35
Fe-Ag	-0.30	-0.30
Fe-Cd	-0.30	-0.30
Fe-Au	-0.32	-0.34
Mn-Cd	-0.31	-0.41
Ru-Au	-0.31	-0.48
Mn-Pt	-0.31	-0.44
Mn-Au	-0.34	-0.65
Rh-Pd	-0.33	-0.95

Table S14. $U_L(V)$ of HER calculated by DFT on 14 potential DMSCs (8 potential DMSCs obtained by ML prediction and 6 potential DMSCs obtained by DFT calculation)

M₁-M₂-N₆-Gra (ML)	ω	$U_L(V)$	M₁-M₂-N₆-Gra (DFT)	ω	$U_L(V)$
Fe-Rh	4	-0.04	Zn-Ru	4	-0.35
Mn-Os	4	-0.32	Co-Au	4	-0.18
Mn-Pd	4	-0.15	Fe-Pd	4	-0.20
Mn-Ru	4	-0.36	Pd-Ir	4	-0.11
Mn-Ir	4	-0.65	Ru-Pt	4	-0.04
Fe-Ag	4	-0.09	Ru-Pd	4	-0.04
Fe-Cd	4	-0.27			
Fe-Au	4	-0.23			

Supporting Figures

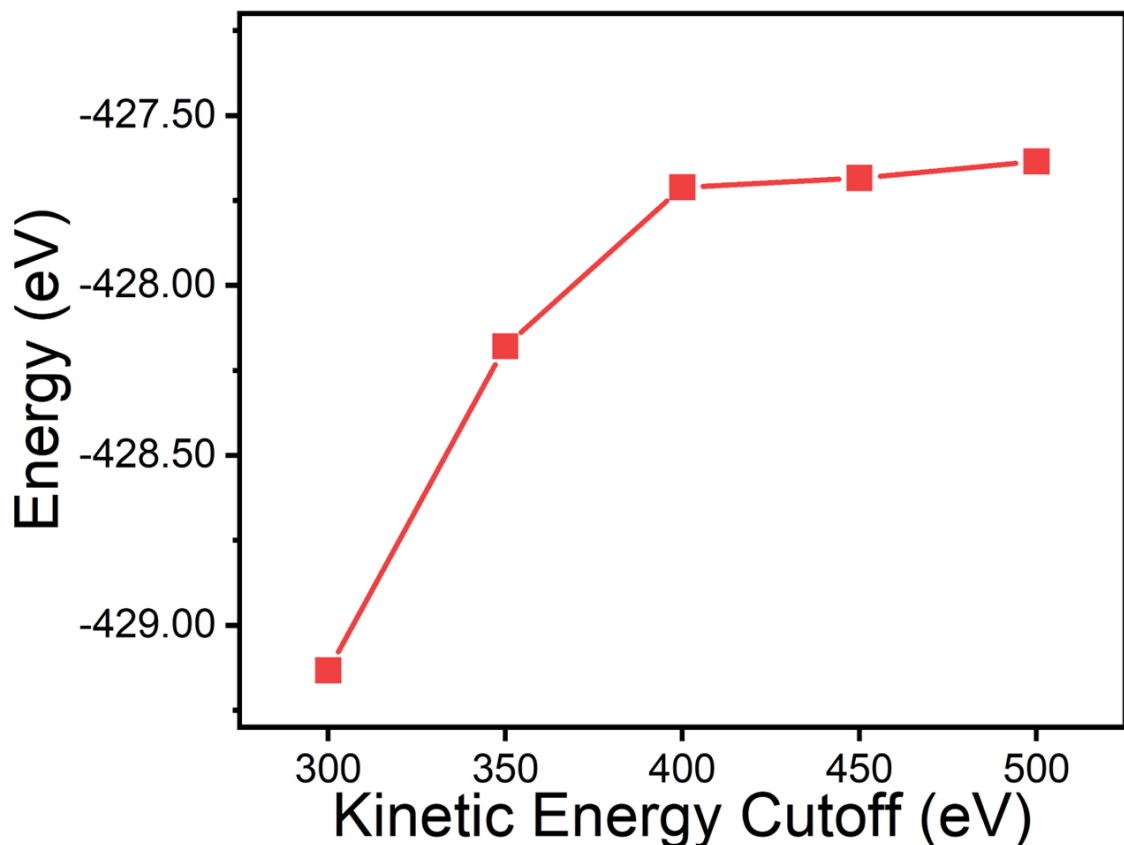


Figure S1. Planewave energy cut off (using $m = 3$ k-points) convergence plots for CO chemisorption on Co-Pt-N₆-Gra model 3.

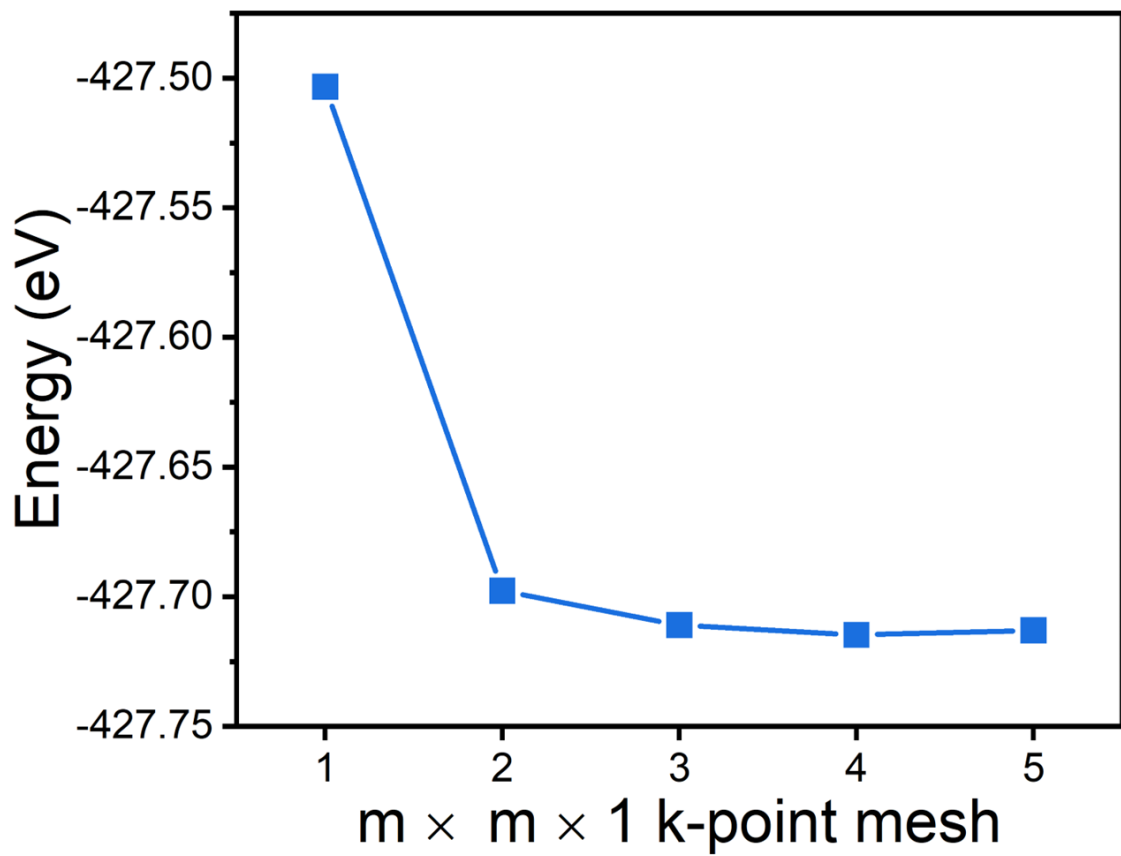


Figure S2. k -point (400 eV cut off) convergence plots for CO chemisorption on Co-Pt-N₆-Gra model 3.

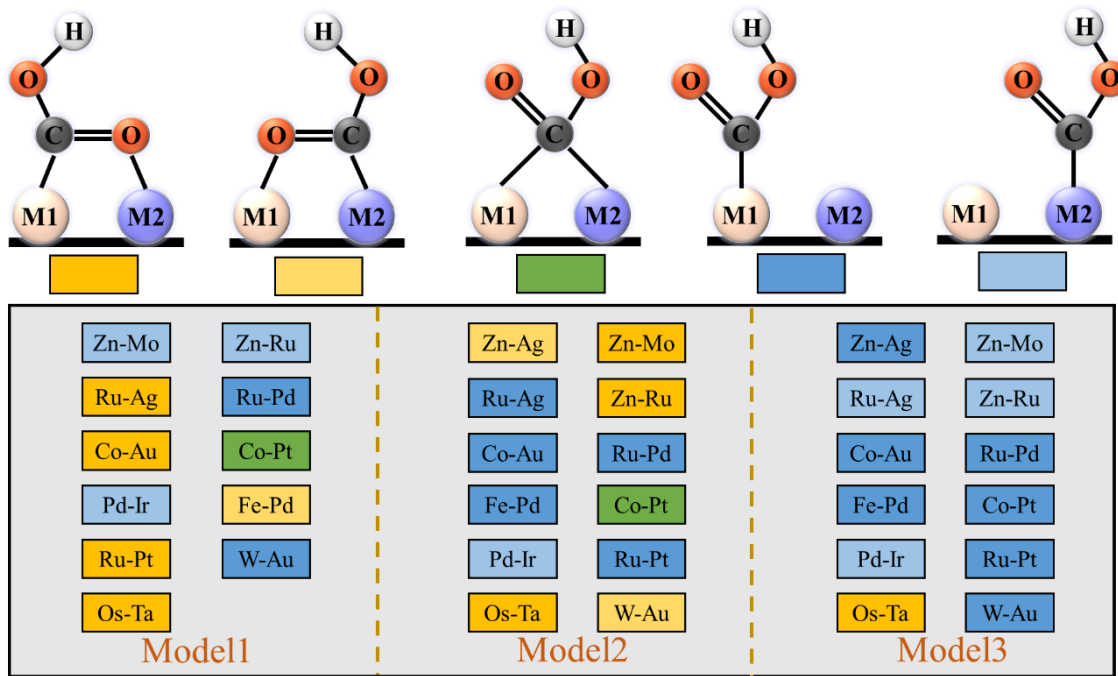


Figure S3. The adsorption configuration of $^*\text{COOH}$ on $\text{M}_1/\text{M}_2\text{-N}_6\text{-Gra}$.

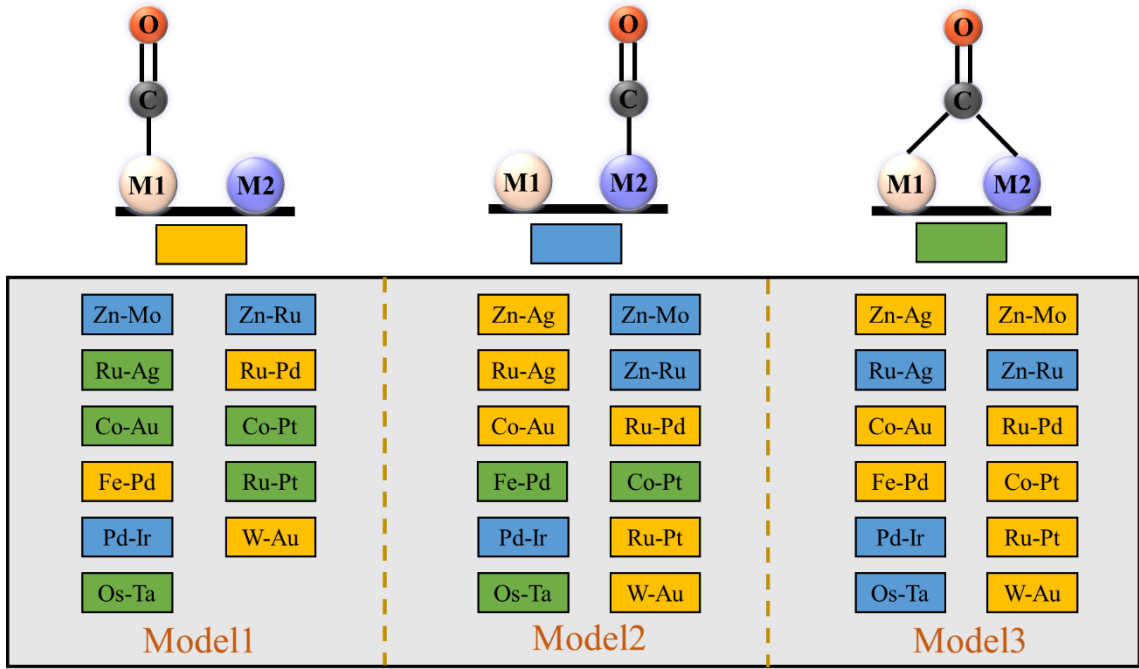


Figure S4. The adsorption configuration of *CO on M₁-M₂-N₆-Gra.

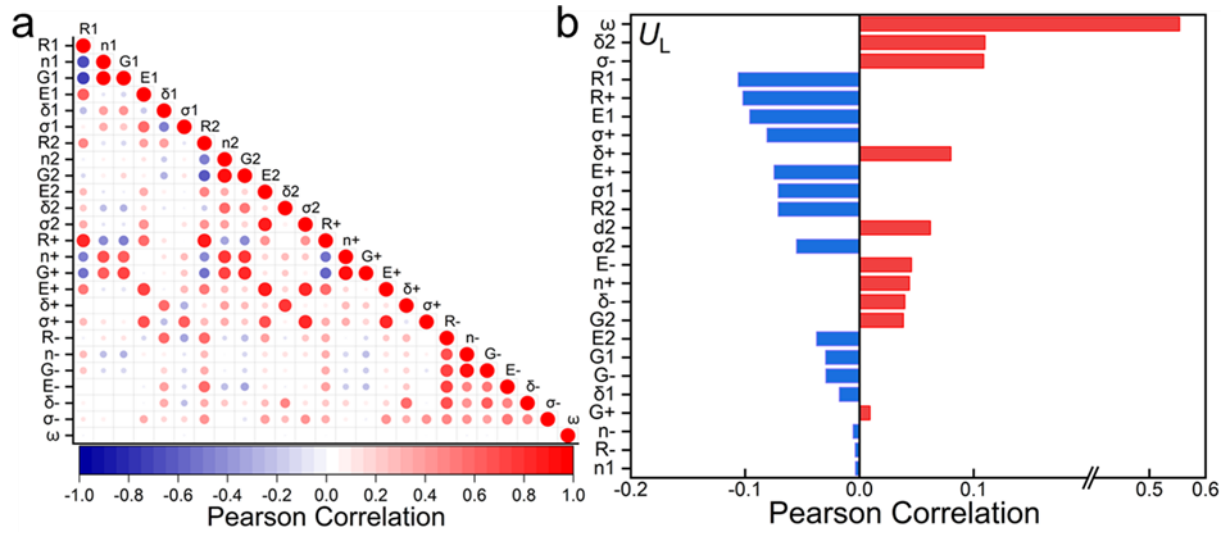


Figure S5. (a) Pearson correlation coefficient matrix heat maps of different initial feature sets. (b) Feature importance rank for the initial descriptor.

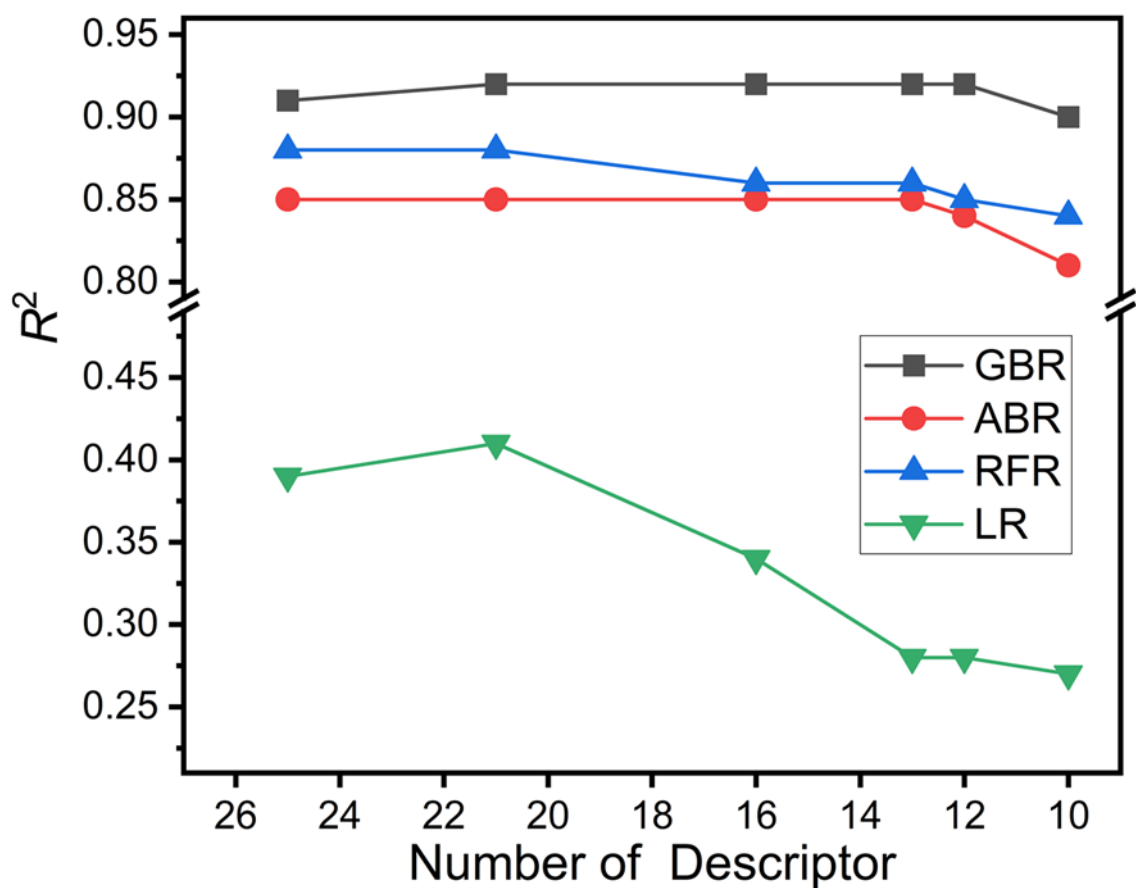


Figure S6. The relationship between R^2 and number of descriptors for four ML models.

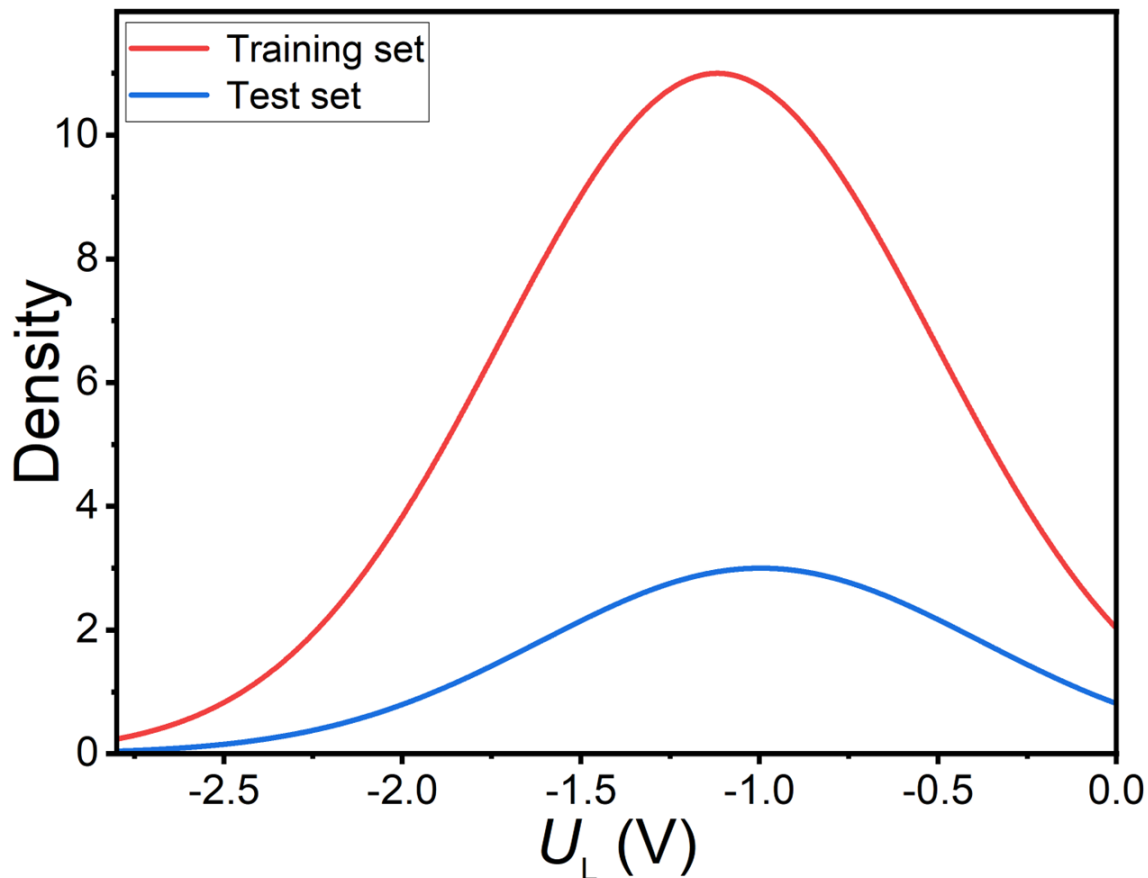


Figure S7. The data distribution of training set and test sets.

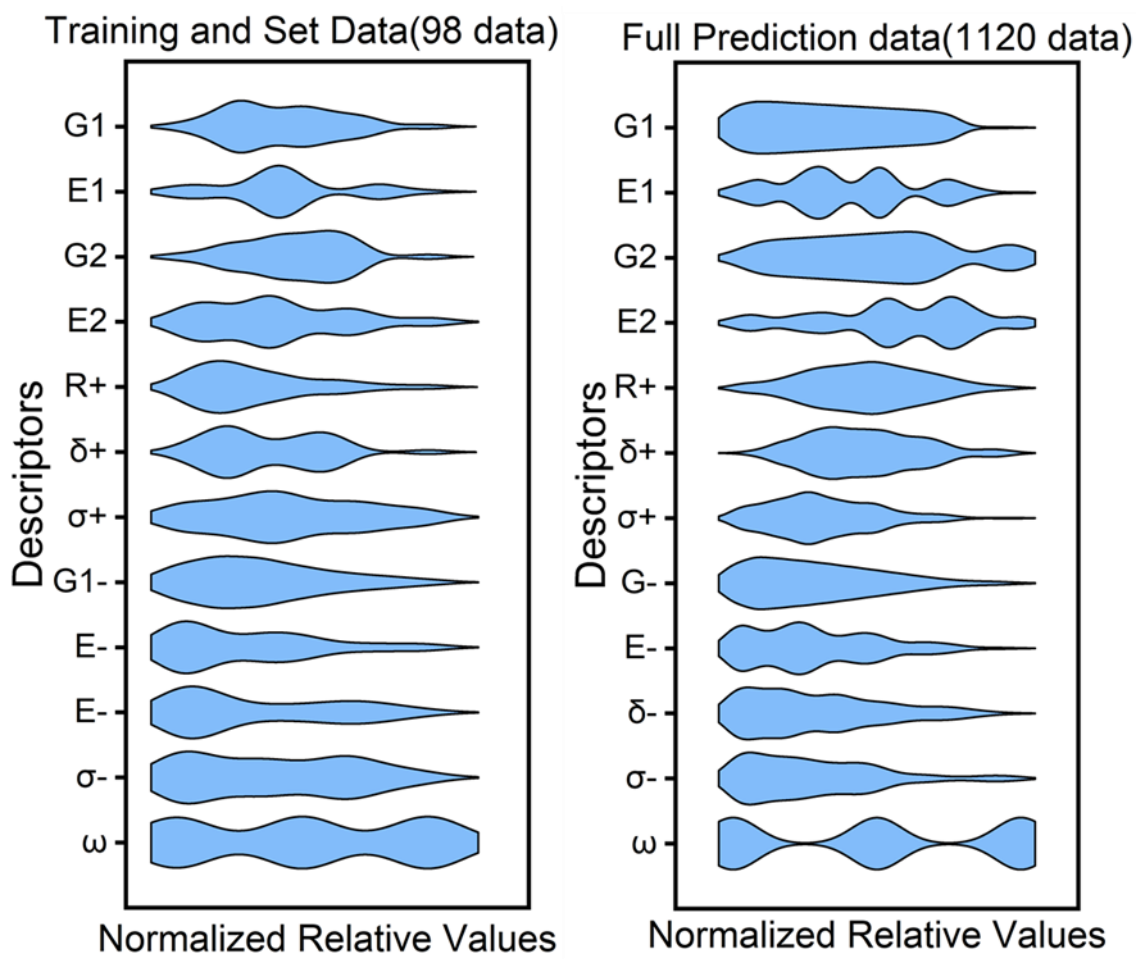


Figure S8. Comparison of the statistical distribution of features (normalized relative values) used in ML model between the training and prediction sets.

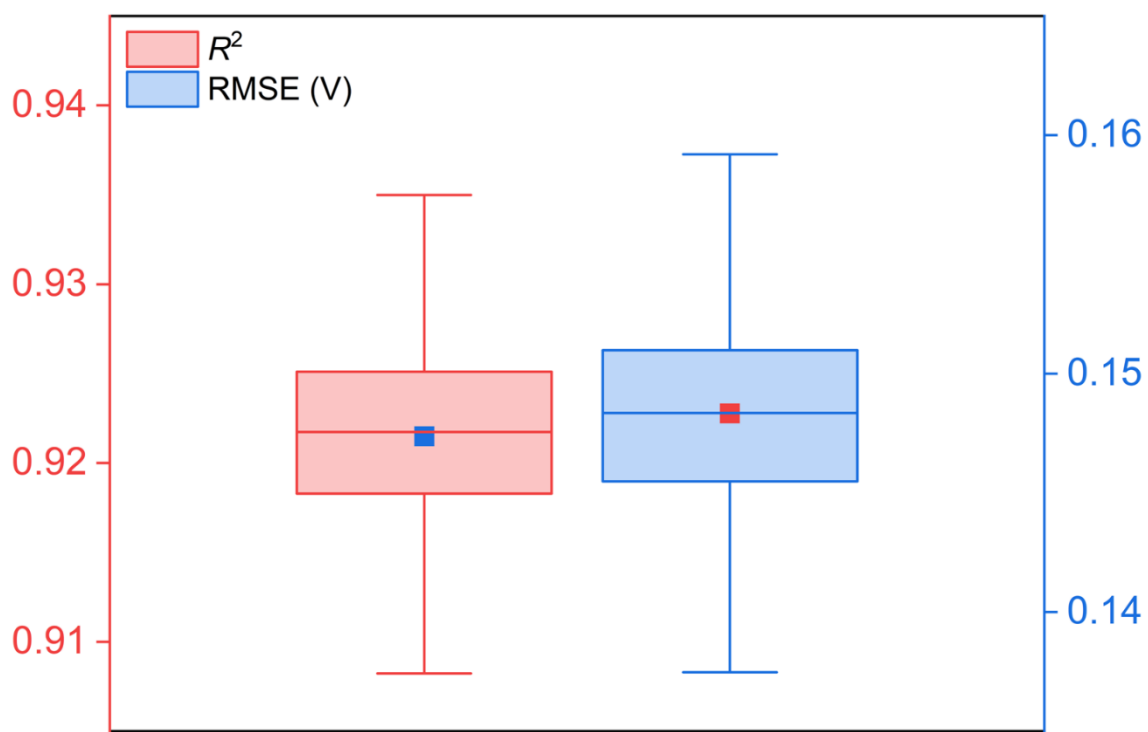


Figure S9. Boxplot of the distribution of the coefficient of determination values (R^2 score) and the root-mean-square error (RMSE) for the GBR model in 1000 trials for 1st round ML.

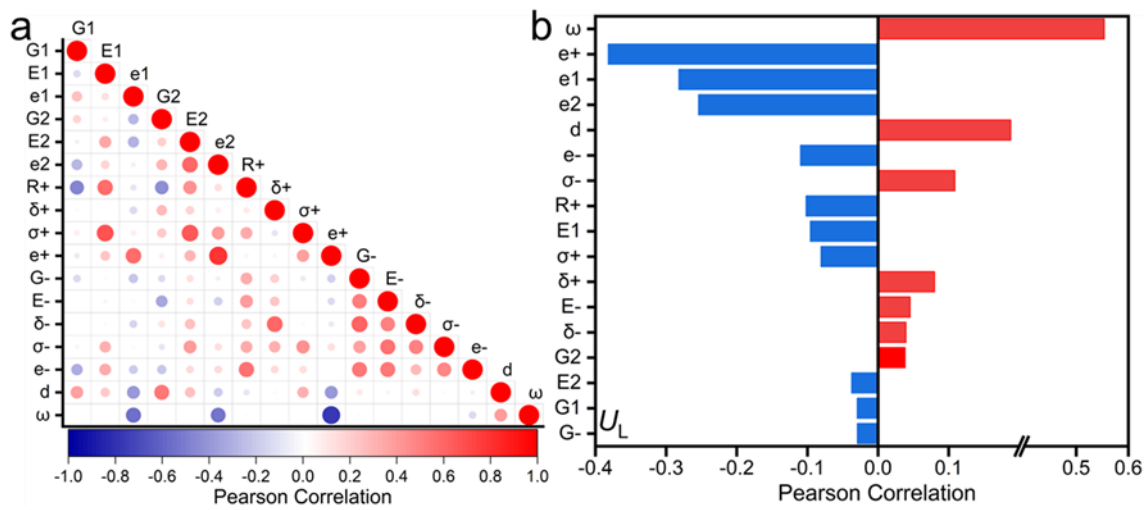


Figure S10. (a) Pearson correlation coefficient matrix heat maps of different feature sets. (b) Feature importance rank for the 17 descriptors in the 2nd ML descriptor.

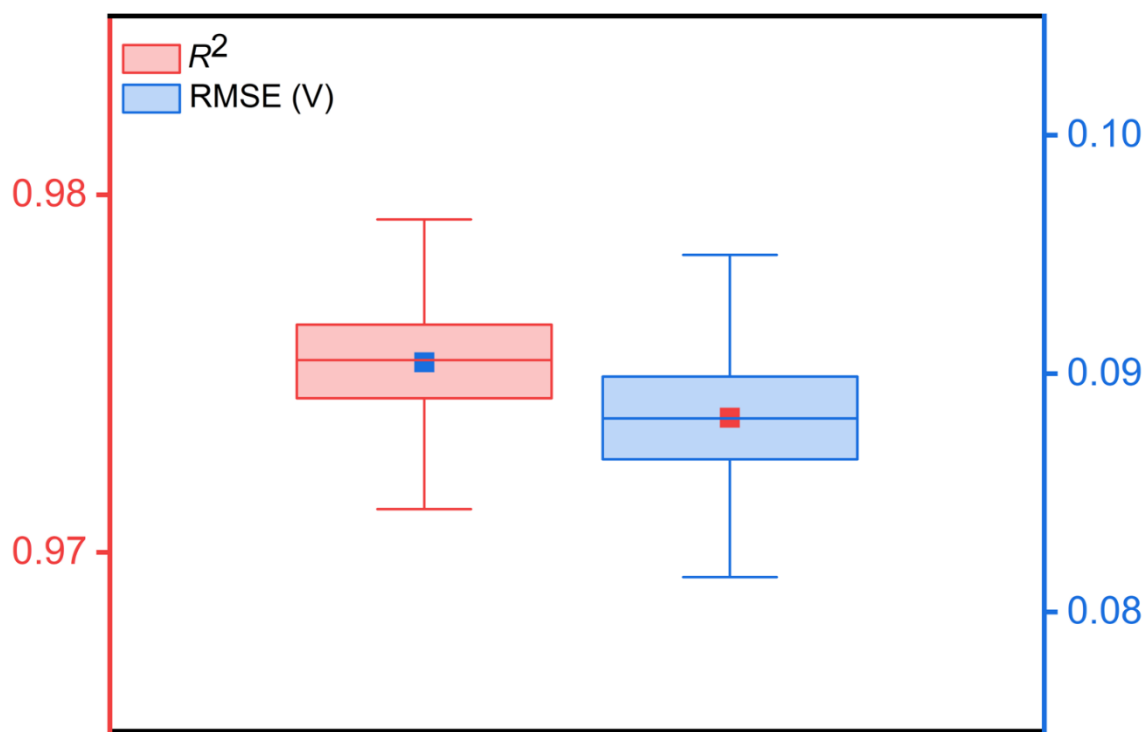


Figure S11. Boxplot of the distribution of the coefficient of determination values (R^2 score) and the root-mean-square error (RMSE) for the GBR model in 1000 trials for 2nd round ML.

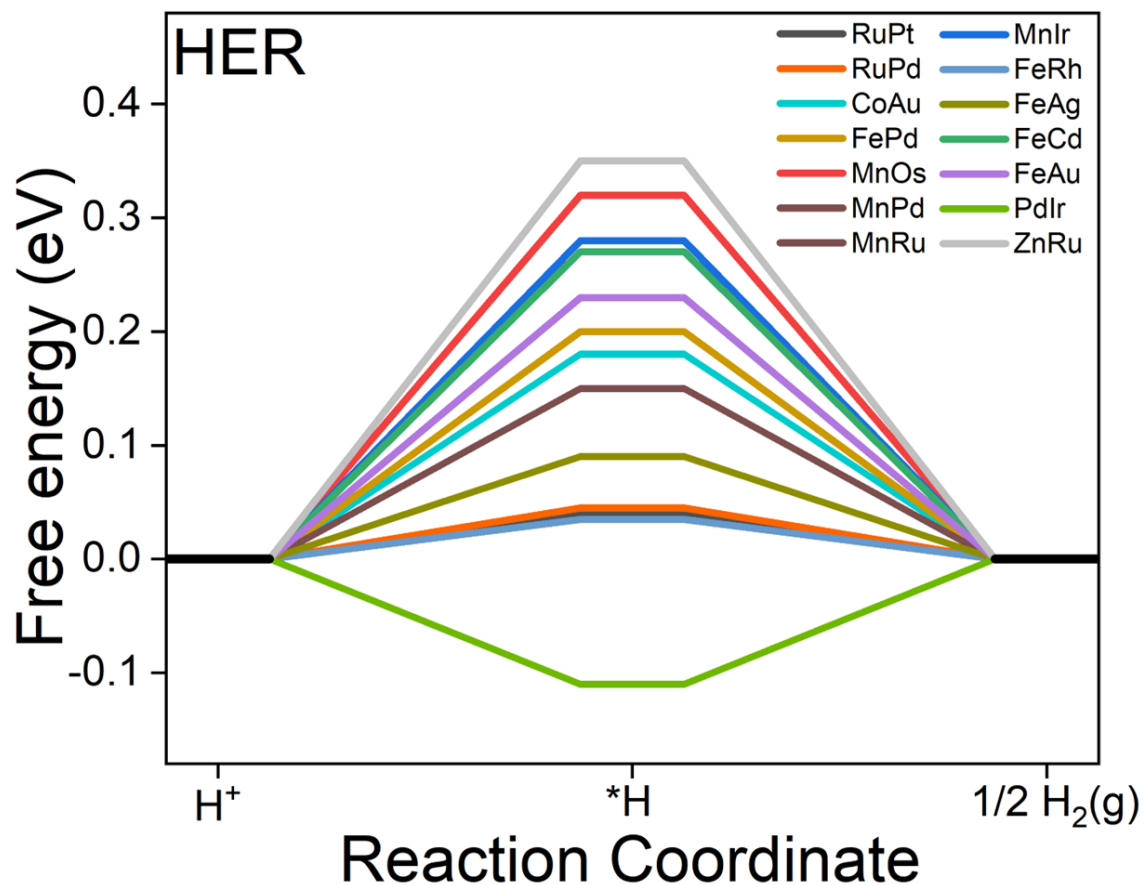


Figure S12. Relative free energy profiles for HER on 14 potential DMSCs (8 potential DMSCs obtained by ML prediction and 6 potential DMSCs obtained by DFT calculation).

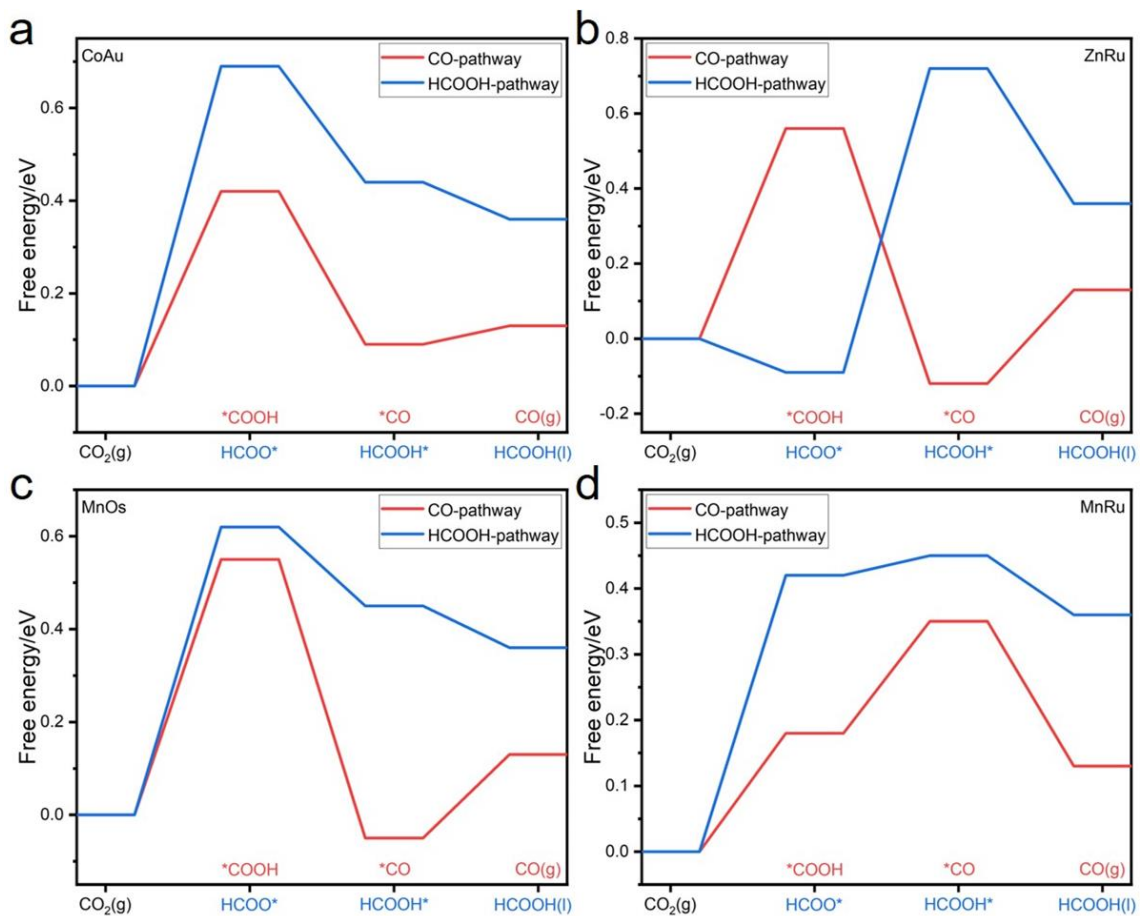


Figure S13. Free energy diagrams for CO_2RR to CO and HCOOH on (a) Co-Au-N₆-Gra-model3, (b) Zn-Ru-N₆-Gra-model3, (c) Mn-Os-N₆-Gra-Model 3, and (d) Mn-Ru-N₆-Gra-Model 3 (solvation correction not performed).

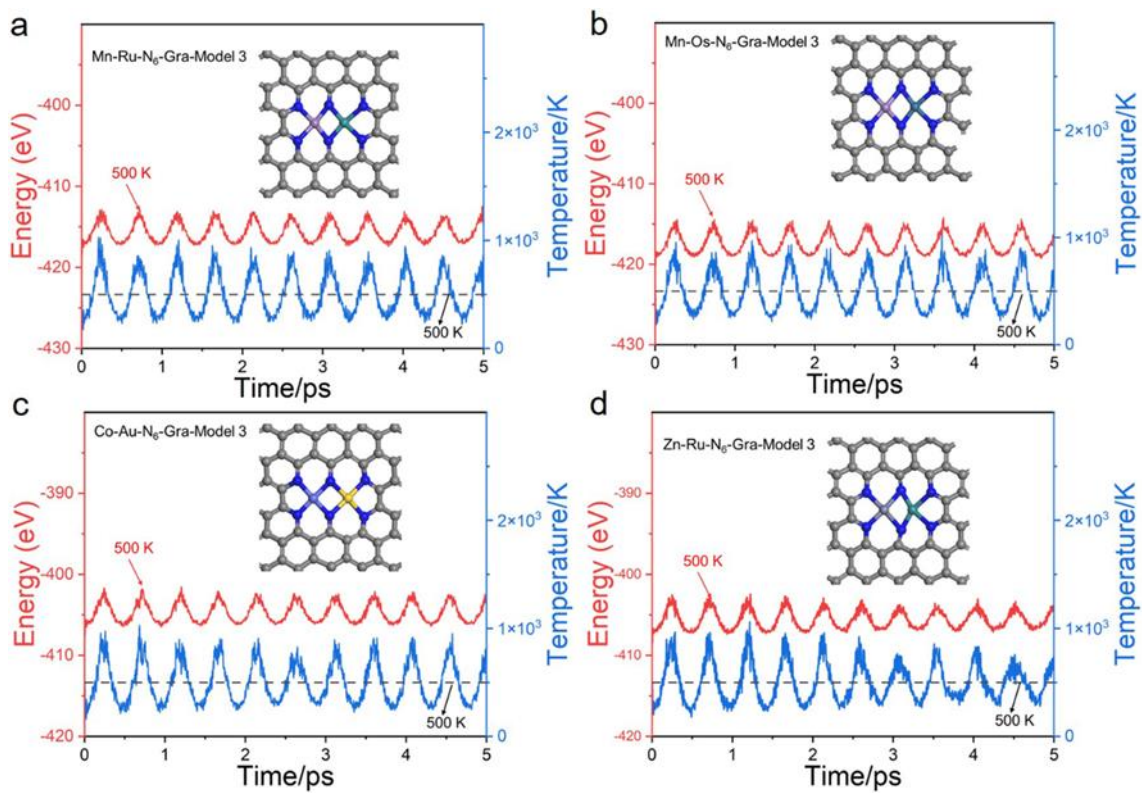


Figure S14. Energy and temperature curves versus the AIMD simulation time for (a) Mn-Ru-N₆-Gra-Model 3, (b) Mn-Os-N₆-Gra-Model 3, (c) Co-Au-N₆-Gra-Model 3, (d) Zn-Ru-N₆-Gra-Model 3.

References

1. Kresse, G.; Furthmiiller, J. *Comput. Mater. Sci.* **1996**, *6*, 15–50.
2. Perdew, J.; Burke, K.; Ernzerhof, M. *Phys. Rev. Lett.* **1996**, *77*, 3865.
3. Kresse, G.; Joubert, D. *Phys. Rev. B: Condens. Matter Mater. Phys.* **1998**, *59*, 1758–1775.
4. Petrilli, H.; Blōchl, P. E.; Blaha, P.; Schwarz, K. *Matter Mater. Phys.* **1998**, *57*, 690–697.
5. Grimme, S.; Antony, J.; Ehrlich, S.; Krieg, H. *J. Chem. Phys.* **2010**, *132*, 154104.
6. Hoover, W. *Phys Rev A*, **1985**, *31*, 1695–1697.
7. He, P.; Feng, H.; Wang, S.; Ding, H.; Liang, Y.; Ling, M.; Zhang, X. *Mater. Adv.* **2022**, *3*, 4566–4577.
8. Nørskov, J.; Rossmeisl, J.; Logadottir, A.; Lindqvist, L. *J. Phys. Chem. B* **2004**, *108*, 17886–17892.
9. Ju, W.; Bagger, A.; Hao, G.; Varela, A.; Sinev, A.; Bon, V.; Cuenya, B.; Kaskel, S.; Rossmeisl, J.; Strasser, P. *Nat. Commun.* **2017**, *8*, 944.
10. Peterson, A.; Abild-Pedersen, F.; Studt, F.; Rossmeisl, J.; Nørskov, J. *Energy Environ. Sci.* **2010**, *3*, 1311–1315.
11. Ren, W.; Tan, X.; Yang, W.; Jia, C.; Xu, S.; Wang, K.; Smith, S.; Zhao, C. *Angew. Chem. Int. Ed.* **2019**, *58*, 6972 –6976.
11. Trucano, P.; Chen, R. *Nature*, **1975**, *258*, 136.